Geodynamic constraints on the steady and time-dependent inner core axial rotation

Mathieu Dumberry

School of Earth and Environment, University of Leeds, Leeds LS2 9JT*, UK. E-mail: dumberry@earth.leeds.ac.uk*

Accepted 2007 May 1. Received 2007 May 1; in original form 2006 October 23

SUMMARY

In this work, constraints on the steady and time-dependent rates of axial inner core rotation are established based on the angular momentum balance between the inner core, fluid core and mantle. It is shown that the rate of a steadily rotating inner core is limited by the torque on the mantle from surface forces at the core–mantle boundary (CMB). The rate of rotation of an oscillating inner core is constrained by the changes in mantle rotation induced by gravitational coupling, which must not exceed the observed changes in length of day. Assuming that the largest torque at the CMB is from electromagnetic forces, our results suggest that the maximum amplitude of an inner core oscillating at a period of 60 yr is $\sim 0.03^\circ$ yr^{-1}, while the maximum amplitude of a steadily rotating inner core is $\sim 0.3^\circ$ yr^{-1}. This implies that the largest inner core rotation rate compatible with the ensemble of seismic studies, 0.2° yr^{-1}, may be explained by a steady rotation but cannot be explained by a decadal oscillation. Though a steady rotation of 0.2° yr^{-1} is possible, it constrains the conductance of the lower mantle to be in the range of 1.6–2.5 $\times$ 10^9 S and the viscous relaxation timescale of the inner core to be in the range of 5–8 yr (i.e. a bulk inner core viscosity of 2.5–4 $\times$ 10^{17} Pa s). Larger steady and oscillating rotation rates may be possible if the inner core can deform on a timescale shorter than $\sim$5 yr or if the conductance of the lower mantle is larger than $\sim 2.5 \times 10^9$ S, though this would then contradict constraints on these two quantities derived from other observations. Finally, we note that a steadily rotating inner core is compatible with the westward motions of magnetic field features at the CMB, as the latter provide the electromagnetic torque on the mantle that balances the gravitational torque from the rotating inner core. In addition, these westward motions must be predominantly due to advection by flow rather than to the propagation of hydromagnetic waves, as the electromagnetic torque at the CMB is otherwise too small to allow an inner core rotation rate as large as 0.2° yr^{-1}.

Key words: Earth's magnetic field, Earth's rotation, inner core, inner core rotation, inner core viscosity.

GJI Tectonics and geodynamics

1 INTRODUCTION

A decade ago, the first efforts in 3-D numerical simulations of the geodynamo suggested that convective flows responsible for maintaining the Earth's magnetic field were entraining the inner core to rotate at a faster rate than the mantle (Glatzmaier & Roberts 1995, 1996). This motivated a number of seismic studies to search for evidence of this. The eastward rotation of the inner core was soon detected by analyses of body waves travelling through the inner core, interpreted to represent a rotation of the orientation of its anisotropic structure (Song & Richards 1996; Su *et al.* 1996). This interpretation was later revised to a shift in time of the lateral velocity gradient within the inner core, from which a rate of rotation of 0.2–0.5° yr^{-1} can be inferred (Creager 1997; Song 2000; Zhang *et al.* 2005). Temporal changes of the scattering caused by small-scale heterogeneity is also indicative of an inner core rotating eastward, albeit at a slightly slower rate (Vidale *et al.* 2000). Analyses of the splitting functions of normal modes rather suggest a non-rotating inner core (Laske & Masters 1999), though a rate of 0.2° yr^{-1} remains marginally compatible with the observations, and may be considered the largest estimate from the ensemble of seismic observations. Recent reviews on the seismically derived inner core rotation rate can be found in Tromp (2001), Song (2003) and Souriau & Poupinet (2003).

Dynamically, a differential rotation of the inner core may result if it is entrained by a torque from surface stresses at the inner core boundary (ICB). The most efficient torque is likely that produced by azimuthal flows near the ICB which, by shearing the magnetic field, lead to an electromagnetic torque that entrains the inner core in the same direction as the flows (Gubbins 1981). An eastward inner core rotation could then result if there exists an eastward flow at the base of the fluid core. This is precisely what is observed in the numerical models of the geodynamo by Glatzmaier & Roberts (1995, 1996). In the models, the mean eastward flow near the ICB is part of a steady azimuthal thermal wind inside the tangent cylinder (the imaginary cylindrical surface tangent to the inner core equator), where the mean azimuthal flow is prograde (eastward) near the ICB, retrograde (westward) near the core–mantle boundary (CMB), and where the poloidal flow is characterized by an upwelling along the rotation axis. Such a 'polar vortex' is a standard feature in many numerical models of the geodynamo (Kono & Roberts 2002) and is also observed in laboratory experiments simulating convection within the tangent cylinder (Aurnou *et al.* 2003). Furthermore, the geomagnetic secular variation at the CMB is consistent with the presence of a polar retrograde flow (Olson & Aurnou 1999; Hulot *et al.* 2002; Holme & Olsen 2006) and the weaker radial magnetic field in the North polar region is consistent with the expulsion of field lines by the upwelling flow (Olson & Aurnou 1999). Thus, the presence of a thermal wind flow inside the tangent cylinder is supported by theory and observation, and provides a mechanism for the differential rotation of the inner core with respect to the mantle. Indeed, predictions of inner core rotation rates based on this thermal wind mechanism were shown to be consistent with the rates inferred by seismic observations (Aurnou *et al.* 1996, 1998; Hollerbach 1998).

However, a steadily differentially rotating inner core is at odds with the presence of non-axially symmetric mass anomalies in the mantle. The density structure within the inner core is expected to reflect that of the mantle and any axial misalignment between the two should result in a gravitational torque (Buffett 1996). Estimates of the magnitude of this torque suggest that the angle of misalignment can be a fraction of a degree at most. Therefore, no steady differential rotation of the inner core should occur. However, an eastward inner core rotation can still be reconciled with the gravitational torque if the inner core can deform viscously on a relatively short timescale (Buffett 1997). In this viscous scenario, the bulk of the inner core—and the part that carries the seismic signature—is steadily rotating, but continuous viscous relaxation maintains the inner core density structure at a fixed misalignment angle with respect to the mantle. At steady state, the misalignment angle is that which allows a balance between the gravitational torque and the electromagnetic torque driven by thermal wind. While the inner core is allowed to rotate with respect to the mantle, its rate is no longer determined purely by the driving from thermal wind as is the case in the absence of the gravitational torque, but it is now limited by the rate of viscous relaxation (Buffett 1997; Aurnou & Olson 2000). In order to explain a rotation rate of 0.2° yr^{-1}, viscous relaxation must occur on a on a timescale of $\sim$3 yr or shorter (Buffett 1997). An additional dynamic component of the viscous scenario is that the steady misalignment between the inner core and mantle also exerts a steady gravitational torque on the later. This torque must be balanced by a torque from surface forces at the CMB (Buffett & Creager 1999), and this may impose further restriction on the rate of inner core rotation. This was demonstrated in a geodynamo simulation that included gravitational coupling between the inner core and mantle, and where, despite allowing for rapid viscous relaxation of the inner core, the steady inner core rotation rate was only 0.02° yr^{-1}, a fraction of that of the fluid near the ICB, and an order of magnitude too small to explain the largest seismic signal (Buffett & Glatzmaier 2000).

Though the numerical results of Buffett & Glatzmaier (2000) suggest that the steady thermal wind mechanism is not compatible with the observed rotation rate, it is unclear to what degree this is a consequence of the specific parameters of the simulation. Nevertheless, if the observed rotation rate cannot be driven by a thermal wind, then an alternative mechanism must be sought. The numerical results of Buffett & Glatzmaier (2000) revealed that time-dependent electromagnetic torques at the ICB could produce variations in inner core rotation as large as 0.1° yr^{-1} on a timescale of a few decades. This demonstrated the possibility that the seismic observation may be explained by an oscillating inner core which has been rotating on average eastward for the past few decades. This possibility was investigated by Zatman (2003), who used geomagnetic observations as a guide for reconstructing the historical variations in inner core rotation. His model was based on torsional oscillations in the fluid core inverted from the geomagnetic secular variation. Torsional oscillations are decadal azimuthal oscillations of rigid cylindrical surfaces aligned with the rotation axis. They are predicted by theory (Taylor 1963; Braginsky 1970) and have been confirmed by observations (Jault *et al.* 1988; Jackson *et al.* 1993; Zatman & Bloxham 1997). It has been argued that they should fully entrain the inner core (e.g. Braginsky 1970; Mound & Buffett 2003), and therefore, the historical variations in inner core rotation can in principle be recovered from the observed torsional oscillations inside the tangent cylinder. Based on this idea, Zatman (2003) showed that the sense of rotation of the inner core has been generally prograde between 1970 and 1990 at an average rate of 0.1° yr^{-1}, a result that appears consistent with the seismic observations.

The argument of a tight coupling between the torsional oscillations and the inner core is based on electromagnetic coupling alone and neglects gravitational coupling. At short timescales, we expect that the gravitational torque may not prevent an inertially accelerated inner core from rotating with respect to the mantle. The inner core is then free to follow the motion of the fluid. However, at long timescales, a rigid inner core should be gravitationally locked to the mantle, as is the case at steady state. On the one hand, this may prevent the inner core from being entrained by torsional oscillations, in which case the rates derived by Zatman (2003) are overestimated. On the other hand, if torsional oscillations succeed in entraining the inner core, the mantle should be dragged along with it, resulting in no differential rotation between the two, and this would not explain the seismic signal. In order to assess whether torsional oscillations can explain the observed inner core rotation, we must determine correctly the degree to which they entrain the inner core, and the degree to which the latter entrains the mantle.

In addition, and more importantly, the hypothesis of an oscillating inner core, whether driven by torsional oscillations or otherwise, must also be consistent with an observational constraint: the time-dependent changes in mantle rotation induced by gravitational torque must not be larger than the observed changes in length of day (LOD). The largest changes observed in the last few decades are of the order of 3 milliseconds (ms) (e.g. Gross 2001), corresponding to changes in mantle rotation rate of approximately 0.005° yr^{-1}. If the seismically observed rotation rates are due to an oscillating inner core, the later must not entrain the mantle efficiently, or must be allowed to deform viscously on a short timescale. Indeed, Buffett & Creager (1999) showed that if the changes in LOD are entirely due to gravitational coupling, viscous deformations must occur on a timescale of 0.05 yr or shorter in order to permit inner core rotation rates compatible with the seismic observations.

The above considerations suggest that the seismic rates of inner core rotation can be reconciled with either a steadily rotating or an oscillating inner core, but only provided the viscous relaxation timescale of the inner core is relatively short. Yet, a 6-yr oscillation in the LOD has recently been interpreted as a normal mode of gravitational oscillation between the mantle and the inner core (Mound & Buffett 2003, 2006). This interpretation implies that the viscous relaxation timescale must not be smaller than ~5 yr. Given this new constraint, is it still possible to drive inner core rotation rates as large as 0.2° yr^{-1}?

In this paper, we revisit the steady and time-dependent part of the inner core axial rotation. We use simple models of angular momentum dynamics to determine the factors that control the rate of steady inner core rotation driven by a thermal wind. We also use an angular momentum approach to assess how efficiently torsional oscillations can entrain the inner core, how tightly coupled the latter is to the mantle, and the limits on time-dependent inner core rotation such that the changes in mantle rotation do not exceed the observed changes in LOD.

2 STEADY INNER CORE ROTATION

We explore first the possibility that the observed eastward inner core rotation is sustained by a dynamic steady-state balance. We consider the problem from an angular momentum perspective. The equations governing the axial angular momentum of the mantle, the inner core and the fluid core are given, respectively, by

$$\frac{d}{dt} C_m \Omega_m = \Gamma_{\rm cmb} - \Gamma_g, \tag{1}$$

$$\frac{d}{dt} C_i \Omega_i = \Gamma_{\rm icb} + \Gamma_g, \tag{2}$$

$$\frac{d}{dt} \int_V c_f\, \omega_f\, dV = -\Gamma_{\rm cmb} - \Gamma_{\rm icb}, \tag{3}$$

where C_m and C_i are, respectively, the axial moments of inertia of the mantle and inner core, c_f is an axial moment of inertia density within the volume V of the fluid core, Ω_m, Ω_i and ω_f are, respectively, the departures in angular velocity of the mantle, the inner core and fluid parcels within the fluid core with respect to the mean rotation rate of 1 cycle per day, Γ_g is the gravitational torque exerted by the mantle on the inner core, and $\Gamma_{\rm cmb}$ and $\Gamma_{\rm icb}$ are the torques from surface forces on the mantle and inner core, respectively.

For a small angle of axial misalignment α of the non-axisymmetric part of the density structures of the inner core with respect to that of the mantle, the restoring gravitational torque on the inner core is given by

$$\Gamma_g = -\bar{\Gamma}\alpha, \tag{4}$$

where $\bar{\Gamma}$ is a proportionality constant that may be obtained from a mantle density model (Buffett 1996). The changes in time of the misalignment angle α are related to the differential rotation between the inner core and the mantle, and also on the rate at which viscous relaxation of the inner core allows its density structure to adjust to the misaligned gravitational potential imposed by the mantle. We assume that the inner core deforms as a simple Newtonian viscous fluid, in which case the rate of viscous relaxation is proportional to the misalignment angle. Accordingly, in a reference frame fixed to the mantle, the time-evolution of α is determined by

$$\frac{d\alpha}{dt} = \Omega_i - \frac{\alpha}{\tau}, \tag{5}$$

where τ is the characteristic timescale of viscous relaxation.

We are interested in the steady state balance and we set the d/dt terms in (1)–(3) and (5) to zero. Using (4), this balance is determined by

$$\Gamma_{\rm cmb} + \bar{\Gamma}\alpha = 0, \tag{6}$$

$$\Gamma_{\rm icb} - \bar{\Gamma}\alpha = 0, \tag{7}$$

$$\Gamma_{\rm cmb} + \Gamma_{\rm icb} = 0, \tag{8}$$

$$\alpha - \tau\Omega_i = 0. \tag{9}$$

This simple balance illustrates well some of the points noted by previous authors. First, from (7), the steady angle of misalignment between the inner core and the mantle is that for which the gravitational torque balances the torque from surface forces on the inner core (Buffett 1997; Aurnou *et al.* 1998). Second, from (9), given a specific value for α, the steady rotation rate of the inner core is determined by the rate at which viscous deformation can occur (Buffett 1997; Aurnou & Olson 2000). Third, from (8), that $\Gamma_{\rm cmb}$ and $\Gamma_{\rm icb}$ must be equal and opposite in steady state, consistent with the combination of (6) and (7), which implies that the rate of inner core rotation is also limited by the torque from surface forces on the mantle (Buffett & Creager 1999; Buffett & Glatzmaier 2000).

The torque from surfaces forces at the ICB should be dominated by electromagnetic coupling (e.g. Gubbins 1981; Aurnou & Olson 2000). As we show in Appendix A, when the azimuthal flow inside the tangent cylinder has the profile of a thermal wind, this torque can be written in the form

$$\Gamma_{\rm icb} = r_i^5 \sigma B_r^2 \left[\chi_\beta \left(\Omega_f - \Omega_i\right) - \chi_\gamma \Omega_f\right], \tag{10}$$

where r_i is the radius of the inner core, B_r is the radial component of the magnetic field at the ICB, σ is the electrical conductivity of the core and Ω_f is the mean angular rotation rate of the fluid at the ICB. The χ_β-part of this expression represents the contribution to the torque from the shear of the magnetic field by the velocity discontinuity at the ICB. The χ_γ-part represents the contribution from the shear of the magnetic field elsewhere in the fluid core. For a thermal wind profile, the latter contribution results in a reduction of the efficiency of the flow to drag the inner core (Aurnou *et al.* 1996, 1998; Hollerbach 1998).

We make the reasonable assumption that the largest torque from surface forces at the CMB is also due to electromagnetic coupling. We assume that a conductive layer of thickness Δ and conductivity σ_m is present at the bottom of the mantle, in which case the torque is proportional to the conductance ($\sigma_m\Delta$), to the square of the mean radial magnetic field at the CMB ($\tilde{B}_r$) and to the angular velocity of the flow near the CMB ($\tilde{\Omega}_f$) (e.g. Holme 1998a). Accordingly, we approximate the torque as

$$\Gamma_{\rm cmb} = K r_f^4 \sigma_m \Delta \tilde{B}_r^2 \tilde{\Omega}_f, \tag{11}$$

where r_f is the radius of the fluid core and K is a numerical constant of $\mathcal{O}(1)$ that takes into account the spatial variations of $\tilde{B}_r$ and $\tilde{\Omega}_f$.

Using (10) and (11) in the steady-state angular momentum balance of (6)–(9), we obtain the following conditions for equilibrium

$$\Omega_i = \frac{\Gamma_{\rm icb}}{\tau\bar{\Gamma}} = \left(\frac{\chi_\beta - \chi_\gamma}{\chi_\beta}\right) \frac{\Omega_f}{1+\zeta}, \tag{12}$$

$$\Omega_i = -\frac{\Gamma_{\rm cmb}}{\tau\bar{\Gamma}} = -\frac{K r_f^4 \sigma_m \Delta \tilde{B}_r^2 \tilde{\Omega}_f}{\tau\bar{\Gamma}}, \tag{13}$$

$$\alpha = \tau\Omega_i, \tag{14}$$

where

$$\zeta = \frac{\tau \bar{\Gamma}}{r_i^5 \sigma \bar{B}_r^{\,2} \chi_\beta}. \tag{15}$$

Eq. (12) represents the rate of inner core rotation driven by electromagnetic coupling at the ICB, whereas eq. (13) may be viewed as the restriction on this rate from the mechanical torque on the CMB. Each of these expressions is a necessary condition for angular momentum equilibrium; they must give the same value of Ω_i. Eq. (14) may be considered a diagnostic equation for α for a given value of Ω_i.

The amplitude of Ω_i derived either from (12) or (13) depends on a number of quantities. To give an example of the amplitude of Ω_i as determined from condition (12), we may take $\sigma = 5 \times 10^5$ S m^{-1} (e.g. Gubbins & Roberts 1987), and $B_r = 2$ mT, typical of most numerical simulations of the geodynamo. Estimates of $\bar{\Gamma}$ and τ may be obtained from the observation of the 6-yr oscillation in LOD and its recent interpretation as a free gravitational mode of oscillation between the mantle and the inner core (Mound & Buffett 2003, 2006). This imposes a rather strict constraint on $\bar{\Gamma}$, which cannot depart much from 3×10^{20} N m. This also requires that the lower bound for τ is 5 yr. Though τ can be much larger, and we consider it a free variable further below, we take $\tau = 5$ yr for this specific example. We use $\Omega_f = 0.5^\circ$ yr^{-1} based on typical thermal wind velocity estimates inside the tangent cylinder (Olson & Aurnou 1999; Hulot *et al.* 2002). Numerical values for χ_β and χ_γ may be obtained by specifying a flow geometry inside the core acting on a prescribed poloidal field geometry. We present in Appendix A a specific example where we obtain $\chi_\beta = 0.77$ and $\chi_\gamma = 0.34$. Using the parameters listed above, which are summarized in Table 1, we obtain $\Omega_i = 0.28^\circ$ yr^{-1}. This implies $\alpha = 1.4^\circ$ and $\Gamma_{\text{cmb}} = -7.2 \times 10^{18}$ N m.

The amplitude of Ω_i predicted by (13) should give an equivalent value. We take $\tilde{\Omega}_f = -0.2^\circ$ yr^{-1}, approximately equal to the rate of westward drift, and $\tilde{B}_r = 0.4$ mT (Langel & Estes 1982). An estimate of the constant K may be obtained from a time-dependent calculation of the torque for a typical core flow acting on the radial field at the CMB. The calculation of Holme (1998a) gives a time-averaged torque of approximately -10^{18} N m with $\sigma_m \Delta = 3 \times 10^8$ S, and for our estimates of $\tilde{B}_r$ and $\tilde{\Omega}_f$ in (11) this implies $K \approx 1.3$. Further below, we let the conductance be a free parameter, but in order to obtain a value for Ω_i equal to that in the previous example, we require $\sigma_m \Delta = 1.6 \times 10^9$ S.

The amplitude of Ω_i is crucially dependent on the choice of the parameters that enter (12) and (13). In principle, since (12) and (13) must be both simultaneously satisfied, either can be used to establish the limits on the rate of inner core rotation. However, it is more convenient to use condition (13) because $\tilde{B}_r$ and $\tilde{\Omega}_f$ are relatively well constrained from surface observations of the geomagnetic field and its secular variation. This leaves only two unknown quantities, the conductance and the viscous relaxation timescale of the inner core, and both of these quantities may be constrained by other observations. In contrast, many of the quantities that enter (12) are not known from observations, including χ_β, χ_γ, Ω_f and B_r. The values for these quantities listed in Table 1 are based on models of the dynamics, and though these may be of the correct order of magnitude, they are far from exact (e.g. Hollerbach 1998). In addition, if there is a significant contribution from magnetic winds inside the tangent cylinder (Sreenivasan & Jones 2005, 2006), the pattern of zonal flows near the ICB may be more complex, and the expression that we have used for Γ_{icb} may not be correct. By using (13), we thus assume that flows deep inside the core are adjusted such that condition (12) gives an equal value of Ω_i, and we establish the rates of inner core rotation independently of the mechanism which is responsible for driving the inner core rotation, whether it is by a steady thermal wind or otherwise.

In Fig. 1, we present how Ω_i varies as a function of τ and $\sigma_m \Delta$ based on condition (13). The rotation rate of the inner core is proportional to $\sigma_m \Delta$ and inversely proportional to τ, as expected from (13); large amplitudes of rotation can be obtained either from a large $\sigma_m \Delta$ or low τ and, for example, with $\tau = 0.6$ yr and $\sigma_m \Delta = 10^{11}$ S, Ω_i is as large as 100° yr^{-1}. However, to drive such a large rotation rate would require flows near the ICB of similar angular velocity, which is very unlikely. This implies that if our estimates of $\tilde{B}_r$ and

Table 1. Parameters used in calculations.

Parameter	Symbol	Value
Radius of ICB	r_i	1.22×10^6 m
Radius of CMB	r_f	3.48×10^6 m
CMB ratio within tangent cylinder	p	0.063
Radial magnetic field at ICB	B_r	2.0 mT
Radial magnetic field at CMB	$\tilde{B}_r$	0.4 mT
Core conductivity	σ	5×10^5 S m^{-1}
Gravitational torque coefficient	$\bar{\Gamma}$	3.0×10^{20} N m
Mean angular velocity at ICB	Ω_f	0.5° yr^{-1}
Mean angular velocity at CMB	$\tilde{\Omega}_f$	-0.2° yr^{-1}
Coefficient of EM torque at CMB	K	1.3
Coefficient of torque from shear at ICB	χ_β	0.77
Coefficient of torque from ambient B_ϕ	χ_γ	0.34
Axial moment of inertia of		
Mantle	C_m	7.12×10^{37} kg m^2
Inner core	C_i	5.87×10^{34} kg m^2
Fluid within tangent cylinder	C_c	2.27×10^{35} kg m^2
Fluid outside tangent cylinder	C_f	8.91×10^{36} kg m^2

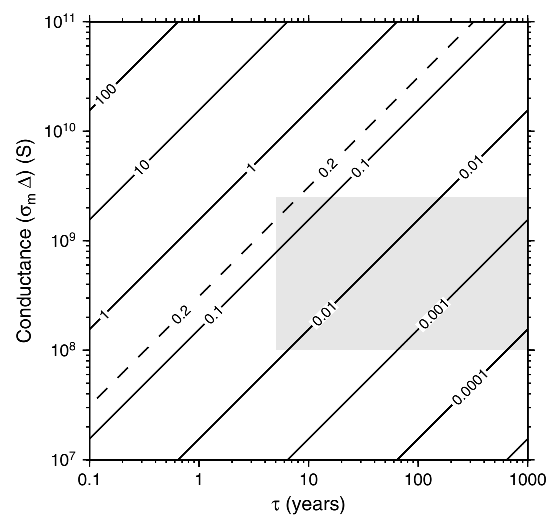

Figure 1. Contours of steady inner core rotation rate (in degrees per year) predicted by (13) as a function of the viscous relaxation timescale τ and conductance of the lower mantle $\sigma_m \Delta$. The other parameters used in the calculations are listed in Table 1. The dashed contour corresponds to 0.2° yr^{-1}, the largest inner core rotation rate compatible with the ensemble of seismic observations. The grey-shaded area marks the region in parameter space compatible with the observation of the 6-yr gravitational mode in the changes in LOD ($\tau > 5$ yr), the forced nutations of the Earth ($\sigma_m \Delta \geq 10^8$ S) and the presence of geomagnetic jerks in the geomagnetic secular variation ($\sigma_m \Delta \leq 2.5 \times 10^9$ S).

$\tilde{\Omega}_f$ are correct, very small values of τ or very large values of $\sigma_m \Delta$ are incompatible with the steady state angular momentum balance. This is consistent with estimates of both τ and $\sigma_m \Delta$ derived from other observations. As mentioned above, the interpretation of the 6-yr oscillation in the LOD as a free gravitational mode establishes a lower bound of $\sim$5 yr for τ. Estimates of the conductance from the observation of forced nutations place a lower bound near 10^8 S (Buffett 1992), but this does not restrict higher values. However, the conductance cannot exceed this value too greatly; the observation of geomagnetic jerks in the secular variation implies that the combination $\mu \sigma_m \Delta^2$, where μ is the permeability of free space, cannot be larger than 0.5 yr (Mandea Alexandrescu *et al.* 1999). Assuming a conductive layer with $\sigma_m = \sigma$, this restriction implies that Δ cannot be larger than 5 km, which imposes an upper limit of $\sigma_m \Delta \leq 2.5 \times 10^9$ S.

The grey-shaded area on Fig. 1 identifies the region of parameter space which is compatible with the above constraints. Rotation rates below 0.1° yr^{-1} can be achieved for a range of different values of τ and $\sigma_m \Delta$. (We note that the very low rotation rates predicted in Fig. 1 would necessarily require that the flows deep in the core must be organized such that Γ_{icb} is much smaller than the prediction we have given above with the parameters in Table 1.) However, large values of Ω_i that are outside the grey-shaded area are not permitted and this allows to place an upper bound on Ω_i. The largest possible steady inner core rotation rate that is not in conflict with the observations of the 6-yr gravitational mode and the geomagnetic jerks is 0.3° yr^{-1}.

The dashed contour on Fig. 1 corresponds to 0.2° yr^{-1}, the largest inner core rotation rate compatible with the ensemble of seismic observations. Although such an amplitude is possible, it imposes rather strict constraints on both τ and $\sigma_m \Delta$. The conductance of the lower mantle must be between $\sim$1.6–2.5 $\times 10^9$ S and the viscous relaxation time of the inner core must be between $\sim 5 - 8$ yr. Using the mapping provided by Buffett (1997), this implies a bulk inner core viscosity of $\eta_s \sim 2.5 - 4 \times 10^{17}$ Pa s. It is important to emphasize that these constraints are independent of the mechanism by which the inner core rotation is driven and rest on the assumption that the dominant torque at the CMB is from electromagnetic forces.

3 TIME-DEPENDENT INNER CORE ROTATION

We expect that decadal variations in inner core rotation are heavily influenced by electromagnetic torques from torsional oscillations and this is the scenario that we explore in this section. As is the case at steady state, when the inner core is rotated out of its axial density alignment with the mantle a gravitational torque acts to resist differential rotation between the two. Unlike at steady-state, changes in rotation rates of the mantle and the inner core may be carried by inertial accelerations and larger rotation rates may be achieved. However, the changes in mantle rotation cannot be larger than those observed as changes in LOD. The goal of this section is to determine whether an inner core entrained by torsional oscillations can oscillate with respect to the mantle with a rotation rate as large as that inferred by seismic observations, while at the same time keeping mantle oscillations within the bounds allowed by changes in LOD. To do this, we build a simplified model of angular momentum dynamics.

Let us assume that time-dependent fluid motion inside the tangent cylinder is comprised of torsional oscillations and, for simplicity, that the departure in angular velocity from a steady mean rotation is everywhere constant and equal to Ω_{c}. In other words, we assume that the whole of the fluid within the tangent cylinder, both above and below the inner core, is rotating as a rigid body. We prescribe a time-dependent torque Γ_{tc} acting on the tangent cylinder which represents the forcing from torsional oscillations in the rest of the fluid core. The equal and opposite torque is acting on the fluid outside the tangent cylinder, which is assumed to rotate rigidly with angular velocity Ω_{o} with respect to a steady mean rotation. The torque Γ_{tc} leads to changes in Ω_c and this in turn entrains the inner core by electromagnetic coupling. The electromagnetic torque on the inner core can be written as (Mound & Buffett 2003)

$$\Gamma_{\mathrm{icb}} = \frac{2\sqrt{2}}{3} \pi r_i^4 B_r^2 \sqrt{\frac{\sigma}{\mu\omega}} (1+i)(\Omega_{\mathrm{c}} - \Omega_i), \tag{16}$$

where ω is the frequency of oscillation. The angular momentum dynamics of the mantle and inner core are governed, respectively, by eqs (1) and (2), which must be supplemented by one equation for the angular momentum of the fluid inside the tangent cylinder, and another one for the fluid outside the tangent cylinder. Using the prescription of the gravitational torque given in (4) and the evolution of the density misalignment angle given in (5), we obtain a linear system describing the evolution of five variables (Ω_m, Ω_i, Ω_c, Ω_{o} and α) as a function of the forcing Γ_{tc},

$$\frac{d}{dt} C_m \Omega_m = \bar{\Gamma}\alpha + \gamma_{\mathrm{c}}[(1-p)\Omega_{\mathrm{o}} + p\Omega_{\mathrm{c}} - \Omega_m], \tag{17}$$

$$\frac{d}{dt} C_i \Omega_i = -\bar{\Gamma}\alpha + \frac{\gamma_i(1+i)}{\sqrt{\omega}}(\Omega_{\mathrm{c}} - \Omega_i), \tag{18}$$

$$\frac{d}{dt} C_{\mathrm{c}} \Omega_{\mathrm{c}} = -\frac{\gamma_i(1+i)}{\sqrt{\omega}}(\Omega_{\mathrm{c}} - \Omega_i) - \gamma_{\mathrm{c}} p(\Omega_{\mathrm{c}} - \Omega_m) + \Gamma_{\mathrm{tc}}, \tag{19}$$

$$\frac{d}{dt} C_{\mathrm{o}} \Omega_{\mathrm{o}} = -\gamma_{\mathrm{c}}(1-p)(\Omega_{\mathrm{o}} - \Omega_m) - \Gamma_{\mathrm{tc}}, \tag{20}$$

$$\frac{d}{dt}\alpha = \Omega_i - \Omega_m - \frac{\alpha}{\tau}, \tag{21}$$

where C_c and C_{o} are, respectively, the axial moments of inertia of the fluid inside and outside the tangent cylinder, $p = 0.063$ is the fraction of the CMB inside the tangent cylinder, and

$$\gamma_c = K\sigma_m \Delta r_f^4 \tilde{B}_r^2, \tag{22}$$

$$\gamma_i = \frac{2\sqrt{2}}{3}\pi r_i^4 B_r^2 \sqrt{\frac{\sigma}{\mu}}. \tag{23}$$

In Section 2, we had defined the various rotation rates with respect to a frame rotating with the mantle. Here, it is more convenient to consider the rotation rate of each region with respect to a frame rotating at a constant mean angular velocity. This is why an additional Ω_m term appears in (17) and (21) compared to their equivalent expressions in Section 2. We specify a periodic forcing of the form $e^{-i\omega t}$, so that $\Gamma_{tc}(t) = \Gamma_{tc} e^{-i\omega t}$, and assume that the response of each variable also has a time-dependency of the same form [i.e. $\Omega_i(t) = \Omega_i\, e^{-i\omega t}$, etc.]. Solutions of the above system are found for given values of ω and are proportional to the amplitude of Γ_{tc}. A more complete model would allow variations in angular velocity as a function of cylinder radius in the fluid both inside and outside the tangent cylinder (Mound & Buffett 2003, 2005). However, this simple model is sufficient to reveal the important aspects of the angular momentum balance and to estimate the amplitude of the changes in inner core rotation that can be driven by torsional oscillations.

Our main objective is to determine the upper bound on the amplitude of inner core oscillations such that the resulting mantle accelerations are not in conflict with the observed changes in LOD. The largest decadal changes in LOD recorded over the last two centuries are of the order of 3 ms, though changes of 1 ms are more typical of the last 60 yr (e.g Gross 2001). This corresponds to maximum changes in mantle rotation of order $0.005^\circ\ \mathrm{yr}^{-1}$, and changes that are three times smaller in the last few decades. Though the observed variations in LOD depend on frequency, for simplicity we take $0.005^\circ\ \mathrm{yr}^{-1}$ as an upper bound for variations in mantle rotation at all frequencies. The largest amplitude of oscillation of each region allowed by the observed LOD changes is then obtained by rescaling the results of our linear system in (17)–(21) by a factor $0.005/|\Omega_m|$. Our results are then independent of the amplitude of the forcing Γ_{tc}. The seismic observations gives the inner core rotation as seen from a frame fixed to the mantle, and so the upper bound in the amplitude of inner core oscillation allowed by the observed LOD changes is given by $|\hat{\Omega}_i| = 0.005 \times (|\Omega_i|/|\Omega_m| - 1)$.

In Figs 2 and 3, we show how $|\hat{\Omega}_i|$ varies as a function of $\sigma_m\Delta$ and τ, respectively, and as a function of the period of oscillation. In each of these figures, we have used the parameters listed in Table 1, with $\tau = 5$ yr (Fig. 2) and $\sigma_m\Delta = 2.5 \times 10^9$ S (Fig. 3). The 'softer' the inner core is, the larger the amplitude of inner core oscillation with respect to the mantle can be. Thus, the contours on Fig. 2 represent the largest amplitudes of inner core oscillation that are compatible with the 6-yr free gravitational mode. Similarly, the larger the torque on the mantle at the CMB is, the more the gravitational torque from the inner core may be offset and the larger the amplitude of inner core oscillation can be. By selecting $\sigma_m\Delta = 2.5 \times 10^9$ S in Fig. 3, these contours represent the largest amplitudes of inner core oscillation that are compatible with the geomagnetic jerks.

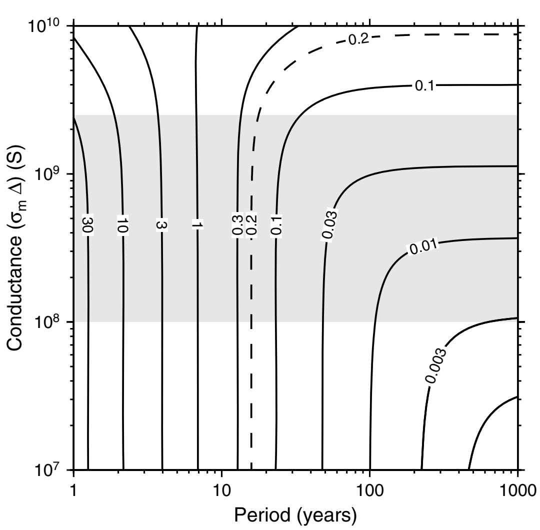

Figure 2. Contours of the maximum rates of differential inner core rotation (in degrees per year) as a function of the period of oscillation and the conductance of the lower mantle $\sigma_m\Delta$. The maximum rate is define as that which produces a change in LOD equal to 3 ms, and is calculated according to $|\hat{\Omega}_i| = 0.005 * (|\Omega_i|/|\Omega_m| - 1)$. The dashed contour corresponds to $0.2^\circ\ \mathrm{yr}^{-1}$, the largest inner core rotation rate compatible with the ensemble of seismic observations. These results have been obtained with the parameters in Table 1, and $\tau = 5$ yr. The grey-shaded area delimits the values of conductance that are compatible with the forced nutations of the Earth ($\sigma_m\Delta \geq 10^8$ S) and the presence of geomagnetic jerks in the geomagnetic secular variation ($\sigma_m\Delta \leq 2.5 \times 10^9$ S).

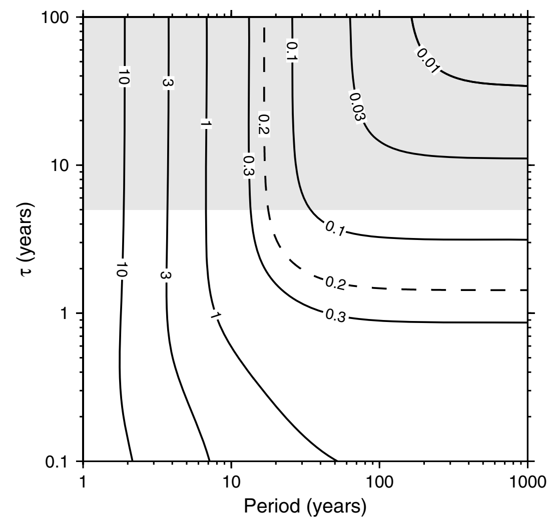

Figure 3. Contours of the maximum rates of differential inner core rotation (in degrees per year) as a function of the period of oscillation and the viscous relaxation timescale of the inner core τ. The maximum rate is define as that which produces a change in LOD equal to 3 ms, and is calculated according to $|\hat{\Omega}_i| = 0.005 * (|\Omega_i|/|\Omega_m| - 1)$. The dashed contour corresponds to $0.2^\circ\ \mathrm{yr}^{-1}$, the largest inner core rotation rate compatible with the ensemble of seismic observations. These results have been obtained with the parameters in Table 1, and $\sigma_m\Delta = 2.5 \times 10^9$ S. The grey-shaded area delimits the values of τ compatible with the observation of the 6-yr gravitational mode in the changes in LOD ($\tau > 5$ yr).

In both Figs 2 and 3, we have included a grey-shaded area that delimits the same bounds on $\sigma_m\Delta$ and τ that we have used in Fig. 1. The results in Figs 2 and 3 can then be used to determine the upper bound of the angular velocity of an oscillating inner core at a given periodicity. At periods of 10 yr or less, because the mantle is not efficiently entrained gravitationally by the inner core, inner core oscillations with amplitude larger than $0.5^\circ\ \mathrm{yr}^{-1}$ do not produce changes in mantle rotation in excess of $0.005^\circ\ \mathrm{yr}^{-1}$ (or a 3 ms change in LOD). We note that the observed changes in LOD at subdecadal periods are much less than 3 ms; the limit on Ω_i at subdecadal periods is probably closer to $1^\circ\ \mathrm{yr}^{-1}$ rather than the large values shown in Figs 2 and 3. $|\hat{\Omega}_i|$ decreases with an increase in the period because the inner core entrains the mantle with greater efficiency. The largest seismically inferred rate of $0.2^\circ\ \mathrm{yr}^{-1}$, indicated by the dashed contour, can be explained by an oscillating inner core, but only provided the period of oscillation is smaller than 15 yr. If we use the more restrictive upper bound of 1 ms change in LOD, the period of oscillation must be below 9 yr. However, the seismic observations are more suggestive of a rotation in one specific direction during the last 30 yr, if not much longer. The rapid decrease in $|\hat{\Omega}_i|$ with periods is such that a slow oscillating inner core is not compatible with the largest seismic rotation rates. For instance, at periods of 60 yr, the upper bound for the rotation rate of an oscillating inner core is closer to $0.03^\circ\ \mathrm{yr}^{-1}$, an order of magnitude too small.

In order to have $|\hat{\Omega}_i| = 0.2^\circ\ \mathrm{yr}^{-1}$ at periods of 60 yr, either a conductance as large as 8×10^9 S is required (see Fig. 2), or τ must be smaller than 1.3 yr (see Fig. 3). If we use the more restrictive upper bound of 1 ms change in LOD, then an amplitude of inner core rotation of $0.2^\circ\ \mathrm{yr}^{-1}$ requires $\sigma_m\Delta \sim 2.4 \times 10^{10}$ S—much larger than allowed by the observation of geomagnetic jerks—or $\tau \sim 0.4$ yr—much smaller than the lower bound allowed by the observation of the 6-yr gravitational mode. While it is marginally possible to explain a steady rotation rate of $0.2^\circ\ \mathrm{yr}^{-1}$, it is not possible to explain such a rate with an inner core oscillating at periods of a few decades as this would result in larger changes in LOD than those observed. More rapid oscillations (periods <10 yr) of amplitudes as large as 0.2° yr^{-1} are not in conflict with the LOD changes. However, the ensemble of seismic observations is unlikely to be solely the result of short-period inner core oscillations: assuming the temporal coverage between all the studies is uniform, we would then expect half of the studies to report a westward rotation. Since nearly all seismic studies find an eastward rotation, it requires the presence of a steady or long-period inner core rotation, though short-period oscillations may be present and influence the results of individual seismic studies.

Though at periods larger than a few decades the inner core oscillation is limited to amplitudes of $\sim 0.03^\circ$ yr^{-1}, at very long periods we should, in principle, recover the steady rotation rates predicted in the previous section. In the balance at steady state, a flow adjustment inside the core must take place for the torque at the ICB to be equal to that at the CMB. Our prescription of the torque at the ICB in (16) does not take such an adjustment into account. Thus, while the form of this torque may be appropriate for decade periods, it is likely no longer valid at periods longer than a few hundred years, and our simple model cannot be used to recover the rotation rates predicted at steady state.

We have assumed here that the inner core oscillation is driven by torsional oscillations and the predicted upper bounds for Ω_i that are shown in Figs 2 and 3 are dependent on the details of our simple model. However, it is important to emphasize that even if the inner core is rotationally accelerated by a different mechanism, it would still exert a gravitational torque on the mantle, and thus its amplitude of oscillation would still be constrained by the observed changes in the LOD. Thus we expect that the conclusion we have derived above are general, unless there exists a time-dependent torque at the CMB of a much larger amplitude than that from electromagnetic stresses.

4 DISCUSSION AND CONCLUSION

We have shown that the rate of a steadily rotating inner core driven by thermal wind is limited by the torque that the flow near the CMB can exert on the mantle, while the amplitude of an oscillating inner core is limited by the observed changes in LOD. The maximum rate of steady rotation is $\sim 0.3^\circ$ yr^{-1}. This suggests that the largest inner core rotation rate compatible with the ensemble of seismic studies, 0.2° yr^{-1}, can be explained by a steadily rotating inner core, though this requires the conductance of the lower mantle to be in the range of 1.6–2.5 $\times 10^9$ S and the viscous relaxation timescale of the inner core to be in the range of 5–8 yr (i.e. a bulk inner core viscosity of 2.5–4 $\times 10^{17}$ Pa s). The maximum amplitude of an oscillating inner core at a period of 60 yr is $\sim 0.03^\circ$ yr^{-1}. Thus, a rate of inner core rotation of 0.2° yr^{-1} is unlikely the result of a decadal inner core oscillation. High-frequency oscillations, with periods shorter than $\sim$10–15 yr, may have an amplitude of 0.2° yr^{-1} or larger without exceeding the observed changes in LOD. However, it is unlikely that high-frequency oscillations alone can explain the ensemble of seismic observations. Hence, we arrive at the conclusion that a steady rotation driven by thermal wind remains the most likely explanation compatible with the largest of the seismic observations, though the rates inferred in individual seismic studies may contain a non-negligible part from subdecadal inner core oscillations.

Larger steady and oscillating rotation rates may be possible if the inner core can deform on a timescale shorter than $\sim$5 yr. However, a viscous relaxation timescale lower than $\sim$5 yr is incompatible with the interpretation that the 6-yr oscillation in the LOD represents the normal mode of gravitational oscillation between the mantle and the inner core (Mound & Buffett 2003, 2006). Similarly, a mantle conductance larger than $\sim 2.5 \times 10^9$ S would allow larger amplitudes of steady rotation and oscillation. However, such a large conductance would be incompatible with the observation of geomagnetic jerks in the secular variation of the magnetic field.

The above conclusions apply under the assumption that the largest torque at the CMB is from electromagnetic forces. If there exists a larger torque of a different nature, larger steady and oscillating rotation rates may be possible [some studies argue for a large topographic torque (Hide 1969; Jault & Le Mouël 1989), though this remains controversial (Kuang & Bloxham 1997; Kuang & Chao 2001)].

Finally, we return to the angular momentum balance that governs the steady inner core rotation, as it provides an explanation to an old conundrum. Motions of magnetic field features at the CMB are time-dependent and spatially complex. Nevertheless, they are dominated by quasi-steady westward motions in the equatorial region of the Atlantic hemisphere (e.g. Bloxham *et al.* 1989; Finlay & Jackson 2003); the westward drift is the surface expression of the movement of these localized field features. As we have seen, these westward motions at the CMB exert a retrograde electromagnetic torque on the mantle, the amplitude of which is dependent on the mantle conductance. The latter must be balanced by an equal and opposite torque, otherwise the mantle would be steadily accelerating. The original assumption was that the torque from the leakage of the core toroidal field in the mantle provided the balance (Bullard *et al.* 1950; Rochester 1960; Stix & Roberts 1984). However, this requires a very large toroidal field in the core (Love & Bloxham 1994). In a more general approach, Holme (1998a,b) showed that a zero mean electromagnetic torque at the CMB with no involvement of the leakage torque was possible. However, to achieve this necessitates core flows which, while not in conflict with the secular variation, are not required by it. Such requirements on the flow or the toroidal field are not necessary if a thermal wind profile dominates the steady azimuthal flows inside the tangent cylinder, as suggested by observations (Olson & Aurnou 1999; Hulot *et al.* 2002; Holme & Olsen 2006). In this case, the prograde inner core rotation keeps its density at a constant positive misalignment angle, and this exerts a prograde gravitational torque on the mantle. The retrograde electromagnetic torque on the mantle is thus balanced by this gravitational torque (Buffett & Creager 1999; Buffett & Glatzmaier 2000).

We note that a part of the electromagnetic torque occurs naturally as a consequence of this angular momentum balance: the inner core drags the mantle along in its rotation, which implies a differential rotation of the latter with respect to the fluid core. Viewed from the mantle, this implies a bulk westward rotation of the fluid core, and a retrograde electromagnetic torque on the mantle. The dominance of the westward moving features at the CMB would then reflect this bulk differential rotation between the core and mantle. This also provides a justification for core flow inversions in a reference frame drifting with respect to the mantle (e.g. Holme & Whaler 2001).

This interpretation is consistent with the secular variation being dominated by advection of field features by large-scale flows near the CMB, as we have assumed in this study. An alternative interpretation is that the secular variation represents dominantly the phase propagation of hydromagnetic waves (Hide 1966; Braginsky 1967). If this is the case, the propagation of the waves exerts a steady retrograde torque on the mantle (the poloidal torque), though its amplitude is approximately 5 times smaller than the torque from the large-scale flows that we have estimated (e.g. Holme 1998a). This would imply an upper limit on the steady inner core rotation rate of 0.06° yr^{-1}.

A rate as high as $0.2^\circ\ \mathrm{yr}^{-1}$ can only be achieved if the calculation of the electromagnetic torque is based on the assumption of large-scale flows. Thus, the interpretation that the secular variation at the CMB is mostly due to advection by flow is not only consistent with the bulk differential rotation between the fluid core and mantle, it is also consistent with the amplitude of the torque between the two. A torque from hydromagnetic waves may participate in the angular momentum balance, but it is difficult to conceive of a scenario in which this torque would fortuitously provide the exact balance to the gravitational torque. We note finally that concern has been raised regarding the validity of the quasi-steady large-scale flows inverted from the secular variation (Gubbins & Kelly 1996; Love 1999). Here, we have shown that their presence is consistent with the angular momentum balance associated with an eastward rotation of the inner core, and this gives an added degree of confidence in these inverted flows.

ACKNOWLEDGMENTS

I would like to thank Jon Mound for a thorough and constructive review which improved the paper significantly. This work was supported by a NERC postdoctoral fellowship of the UK.

REFERENCES

Aurnou, J. & Olson, P., 2000. Control of inner core rotation by electromagnetic, gravitational and mechanical torques, *Phys. Earth Planet. Inter.,* **117,** 111–121.

Aurnou, J., Andreadis, S., Zhu, L. & Olson, P., 2003. Experiments on convection in Earth's core tangent cylinder, *Earth Planet. Sci. Lett.,* **212,** 119–134.

Aurnou, J.M., Brito, D. & Olson, P.L., 1996. Mechanics of inner core super-rotation, *Geophys. Res. Lett.,* **23,** 3401–3404.

Aurnou, J.M., Brito, D. & Olson, P.L., 1998. Anomalous rotation of the inner core and the toroidal magnetic field, *J. Geophys. Res.,* **103,** 9721–9738.

Bloxham, J., Gubbins, D. & Jackson, A., 1989. Geomagnetic secular variation, *Phil. Trans. R. Soc. Lond., A,* **329,** 415–502.

Braginsky, S.I., 1967. Magnetic waves in the earth's core, *Geomag. Aeron.,* **7,** 851–859.

Braginsky, S.I., 1970. Torsional magnetohydrodynamic vibrations in the Earth's core and variations in day length, *Geomag. Aeron.,* **10,** 1–10.

Buffett, B.A., 1992. Constraints on magnetic energy and mantle conductivity from the forced nutations of the Earth, *J. Geophys. Res.,* **97,** 19 581–19 597.

Buffett, B.A., 1996. Gravitational oscillations in the length of the day, *Geophys. Res. Lett.,* **23,** 2279–2282.

Buffett, B.A., 1997. Geodynamic estimates of the viscosity of the Earth's inner core, *Nature,* **388,** 571–573.

Buffett, B.A. & Creager, K.C., 1999. A comparison of geodetic and seismic estimate of inner-core rotation, *Geophys. Res. Lett.,* **26,** 1509–1512.

Buffett, B.A. & Glatzmaier, G.A., 2000. Gravitational braking of inner-core rotation in geodynamo simulations, *Geophys. Res. Lett.,* **27,** 3125–3128.

Bullard, E.C., Freedman, C., Gellman, H. & Nixon, J., 1950. The westward drift of the Earth's magnetic field, *Phil. Trans. R. Soc. Lond., A,* **243,** 67–92.

Creager, K.C., 1997. Inner core rotation rate from small scale heterogeneity and time-varying travel times, *Science,* **278,** 1284–1288.

Finlay, C.C. & Jackson, A., 2003. Equatorially dominated magnetic field change at the surface of the Earth's core, *Science,* **300,** 2084–2086.

Glatzmaier, G.A. & Roberts, P.H., 1995. A three-dimensional convective dynamo solution with rotating and finitely conducting inner core and mantle, *Phys. Earth Planet. Inter.,* **91,** 63–75.

Glatzmaier, G.A. & Roberts, P.H., 1996. Rotation and magnetism of Earth's inner core, *Science,* **274,** 1887–1891.

Gross, R.S., 2001. A combined length-of-day series spanning 1832–1997: LUNAR97, *Phys. Earth Planet. Inter.,* **123,** 65–76.

Gubbins, D., 1981. Rotation of the inner core, *J. Geophys. Res.,* **86,** 11 695–11 699.

Gubbins, D. & Kelly, P., 1996. A difficulty with using the frozen flux hypothesis to find steady core motions, *Geophys. Res. Lett.,* **23,** 1825–1828.

Gubbins, D. & Roberts, P.H., 1987. Magnetohydrodynamics of the Earth's core, in *Geomagnetism,*Vol. 2, pp. 1–184, ed. Jacobs, J.A., Academic Press, London.

Heerens, W.C., 1976. The solution of Laplace's equation in cylindrical and toroidal configurations with rectangular sectional shapes and rotation-symmetrical boundary conditions, *J. Appl. Phys.,* **47,** 3740–3744.

Hide, R., 1966. Free hydromagnetic oscillations of the Earth's core and the theory of geomagnetic secular variation, *Phil. Trans. R. Soc. Lond., A,* **259,** 615–646.

Hide, R., 1969. Interaction between the Earth's liquid core and solid mantle, *Nature,* **222,** 1055–1056.

Hollerbach, R., 1998. What can the observed rotation of the Earth's inner core reveal about the state of the outer core? *Geophys. J. Int.,* **135,** 564–572.

Holme, R., 1998a. Electromagnetic core-mantle coupling–I. Explaining decadal changes in the length of day, *Geophys. J. Int.,* **132,** 167–180.

Holme, R., 1998b. Electromagnetic core-mantle coupling II: Probing deep mantle conductance, in *The Core-Mantle Boundary Region*, Vol. 28 of Geodynamics Series, pp. 139–152, eds Gurnis, M., Wysession, M.E., Knittle, E. & Buffett, B.A., AGU Geophysical Monograph, Washington, DC.

Holme, R. & Olsen, N., 2006. Core surface flow modelling from high-resolution secular variation, *Geophys. J. Int.,* **166,** 518–528.

Holme, R. & Whaler, K.A., 2001. Steady core flows in an azimuthally drifting reference frame, *Geophys. J. Int.,* **145,** 560–569.

Hulot, G., Eymin, C., Langlais, B., Mandea, M. & Olsen, N., 2002. Small-scale structure of the geodynamo inferred from Oersted and Magsat satellite data, *Nature,* **416,** 620–623.

Jackson, A., Bloxham, J. & Gubbins, D., 1993. Time-dependent flow at the core surface and conservation of angular momentum in the coupled core-mantle system, in *Dynamics of the Earth's Deep Interior and Earth Rotation,*Vol. 72, pp. 97–107, eds Le Mouël, J.-L., Smylie, D.E. & Herring, T., AGU Geophysical Monograph, Washington, DC.

Jault, D. & Le Mouël, J.-L., 1989. The topographic torque associated with a tangentially geostrophic motion at the core surface and inferences on the flow inside the core, *Geophys. Atrophys. Fluid Dyn.,* **48,** 273–296.

Jault, D., Gire, C. & Le Mouël, J.-L., 1988. Westward drift, core motions and exchanges of angular momentum between core and mantle, *Nature,* **333,** 353–356.

Kono, M. & Roberts, P.H., 2002. Recent geodynamo simulations and observations of the geomagnetic field, *Rev. Geophys.,* **40**(4), 1013, doi:10.1029/2000RG000102.

Kuang, W. & Bloxham, J., 1997. On the dynamics of topographical core-mantle coupling, *Phys. Earth Planet. Inter.,* **99,** 289–294.

Kuang, W. & Chao, B.F., 2001. Topographic core-mantle coupling in geodynamo modeling, *Geophys. Res. Lett.,* **28,** 1871–1874.

Langel, R.A. & Estes, R.H., 1982. A geomagnetic field spectrum, *Geophys. Res. Lett.,* **9,** 250–253.

Laske, G. & Masters, G., 1999. Limits on differential rotation of the inner core from an analysis of the Earth's free oscillations, *Nature,* **402,** 66–69.

Love, J.J., 1999. A critique of frozen-flux inverse modelling of a nearly steady geodynamo, *Geophys. J. Int.,* **138,** 353–365.

Love, J.J. & Bloxham, J., 1994. Electromagnetic coupling and the toroidal magnetic field at the core-mantle boundary, *Geophys. J. Int.,* **117,** 235–256.

Mandea Alexandrescu, M., Gibert, D., Le Mouël, J.-L., Hulot, G. & Saracco, G., 1999. An estimate of average lower mantle conductivity by wavelet analysis of geomagnetic jerks, *J. Geophys. Res.,* **104,** 17 735–17 740.

Mound, J.E. & Buffett, B.A., 2003. Interannual oscillations in the length of day: implications for the structure of mantle and core, *J. Geophys. Res.,* **108**(B7), 2334, doi:10.1029/2002JB002054.

Mound, J.E. & Buffett, B.A., 2005. Mechanisms of core-mantle angular momentum exchange and the observed spectral properties of torsional oscillations, *J. Geophys. Res.,* **110,** B08 103, doi:10.1029/2004JB003555.

Mound, J.E. & Buffett, B.A., 2006. Detection of a gravitational oscillation in length-of-day, *Earth Planet. Sci. Lett.,* **243,** 383–389.

Olson, P. & Aurnou, J., 1999. A polar vortex in the Earth's core, *Nature,* **402,** 170–173.

Rochester, M.G., 1960. Geomagnetic westward drift and irregularities in the Earth's rotation, *Phil. Trans. R. Soc. Lond., A,* **252,** 531–555.

Song, X., 2000. Joint inversion for inner core rotation, inner core anisotropy and mantle heterogeneity, *J. Geophys. Res.,* **105,** 7931–7943.

Song, X., 2003. Three-dimensional structure and differential rotation of the inner core, in *Earth's Core: Dynamics, Structure, Rotation*, Vol. 31 of Geodynamics Series, pp. 45–64, eds Dehant, V., Creager, K.C., Karato, S.-I. & Zatman, S., AGU Geophysical Monograph.

Song, X. & Richards, P.G., 1996. Seismological evidence for differential rotation of the Earth's inner core, *Nature,* **382,** 221–224.

Souriau, A. & Poupinet, G., 2003. Inner core rotation: a critical appraisal, in *Earth's Core: Dynamics, Structure, Rotation*, Vol. 31 of Geodynamics Series, pp. 65–82, eds Dehant, V., Creager, K.C., Karato, S.-I. & Zatman, S., AGU Geophysical Monograph.

Sreenivasan, B. & Jones, C.A., 2005. Structure and dynamics of the polar vortex in the Earth's core, *Geophys. Res. Lett.,* **32,** L20 301, doi:10.1029/2005GL023841.

Sreenivasan, B. & Jones, C.A., 2006. Azimuthal winds, convection and dynamo action in the polar regions of planetary cores, *Geophys. Atrophys. Fluid Dyn.,* **100,** 319–339.

Stix, M. & Roberts, P.H., 1984. Time-dependent electromagnetic core-mantle coupling, *Phys. Earth Planet. Inter.,* **36,** 49–60.

Su, W.J., Dziewonski, A.M. & Jeanloz, R., 1996. Planet within a planet: Rotation of the inner core of the Earth, *Science,* **274,** 1883–1887.

Taylor, J.B., 1963. The magneto-hydrodynamics of a rotating fluid and the Earth's dynamo problem, *Proc. R. Soc. Lond., A,* **274,** 274–283.

Tromp, J., 2001. Inner-core anisotropy and rotation, *Ann. Rev. Earth Planet. Sci.,* **29,** 47–69.

Vidale, J.E., Dodge, D.A. & Earle, P.S., 2000. Slow differential rotation of the Earth's inner core indicated by temporal changes in scattering, *Nature,* **405,** 445–448.

Zatman, S., 2003. Decadal oscillations of the Earth's core, angular momentum exchange, and inner core rotation, in *Earth's Core: Dynamics, Structure, Rotation*, Vol. 31 of Geodynamics Series, pp. 233–240, eds Dehant, V., Creager, K.C., Karato, S.-I. & Zatman, S., AGU Geophysical Monograph.

Zatman, S. & Bloxham, J., 1997. Torsional oscillations and the magnetic field within the Earth's core, *Nature,* **388,** 760–763.

Zhang, J., Song, X., Li, Y., Richards, P.G., Sun, X. & Waldhauser, F., 2005. Inner core differential motion confirmed by earthquake waveform doublets, *Science,* **309,** 1357–1360.

APPENDIX A: STEADY ELECTROMAGNETIC TORQUE ON THE INNER CORE

The torque from electromagnetic stresses on the inner core is

$$\Gamma^B_{\text{icb}} = \frac{r_i^3}{\mu} \int_S B_r B_\phi \sin\theta \, dS, \tag{A1}$$

where r_i is the radius of the inner core, μ is the permeability of free space, B_r and B_ϕ are the radial and azimuthal component of the magnetic field at the ICB and S is the surface of the unit sphere. To evaluate this torque, we seek to determine the steady part of B_ϕ produced by the shear of the poloidal field by a steady azimuthal flow. Here, we assume a steady flow which takes the form of a thermal wind prescribed as $\mathbf{v} = v_\phi \hat{\phi}$ with

$$v_\phi = r_i \Omega_f \frac{J_1(\lambda s)}{J_1(c)} \left[1 - \frac{2(z - z_i)}{z_f - z_i} \right], \tag{A2}$$

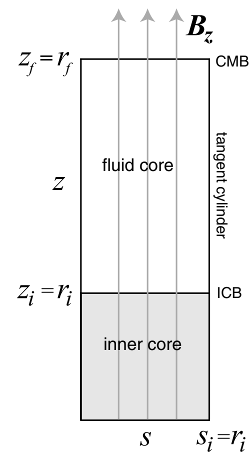

Figure A1. The cylindrical geometry of our idealized calculation. The ICB and CMB correspond respectively at the surfaces $z = z_i = r_i$ and $z = z_f = r_f$, where r_i is the spherical radius of the inner core and r_f that of the fluid core. The tangent cylinder corresponds to the surface $s = s_i = r_i$. An axial magnetic field B_z permeates the whole geometry.

and where Ω_f is the angular rotation rate at the ICB. The functions J_1 are Bessel functions of the first kind and $\lambda = c/r_i$, with $c = 1.843$ chosen so that $\partial v_\phi / \partial s = 0$ at $s = r_i$.

We consider a cylindrical geometry, as depicted in Fig. A1, where the ICB is defined by the surface $z = z_i = r_i$ and the CMB by the surface $z = z_f = r_f$, and where the tangent cylinder is determined by the cylindrical radial surface $s = s_i = r_i$. We assume that the whole geometry is permeated by a uniform axial magnetic field $\mathbf{B} = B_z \hat{\mathbf{z}}$.

Our goal is not to derive the precise value of the torque but rather to identify the components of the dynamics that influence it. With this philosophy in mind, we seek an analytical expression for B_ϕ. Within the fluid, the magnetic field has to obey the steady state induction equation

$$\nabla \times (\mathbf{v} \times \mathbf{B}) + \eta \nabla^2 \mathbf{B} = 0, \tag{A3}$$

where $\eta = 1/\mu\sigma$ and where σ is the electrical conductivity. Using (A2) and the uniform B_z, B_ϕ in the fluid must satisfy the linearized eq. (A3)

$$\frac{\partial^2 B^f_\phi}{\partial s^2} + \frac{1}{s}\frac{\partial B^f_\phi}{\partial s} - \frac{B^f_\phi}{s^2} + \frac{\partial^2 B^f_\phi}{\partial z^2} = \frac{2 r_i \Omega_f B_z J_1(\lambda s)}{\eta (z_f - z_i) J_1(c)}. \tag{A4}$$

In the inner core there is no differential velocity and B^i_ϕ must satisfy the vector Laplacian equation

$$\left(\nabla^2 \mathbf{B}\right)_\phi = \frac{\partial^2 B^i_\phi}{\partial s^2} + \frac{1}{s}\frac{\partial B^i_\phi}{\partial s} - \frac{B^i_\phi}{s^2} + \frac{\partial^2 B^i_\phi}{\partial z^2} = 0. \tag{A5}$$

With the boundary conditions $B_\phi = 0$ at $s = 0$ and $\partial B_\phi / \partial s = 0$ at $s = r_i$, the solution in the inner core and the homogeneous part of the solution in the fluid are of the form (e.g. Heerens 1976)

$$B_\phi = J_1(\lambda s) \left[C_1 \sinh(\lambda z) + C_2 \cosh(\lambda z) \right]. \tag{A6}$$

In the fluid, a particular solution that satisfies the right-hand side of (A4) must be added to the homogeneous part. Due to our convenient choice for the thermal wind, this solution follows the same radial dependency as the homogeneous part, and is given by

$$B_\phi = -\frac{2 r_i \Omega_f B_z J_1(\lambda s)}{\lambda^2 \eta (z_f - z_i) J_1(c)}. \tag{A7}$$

The four constants of integration in (A6) (2 in each region) are determined by four boundary conditions. The first 3 are that B_ϕ must vanish at $z = 0$ and $z = z_f$, and must be continuous at $z = z_i$. The fourth condition is the requirement that the tangential electric field is continuous at the ICB, which relates the discontinuity in the vertical gradient of B_ϕ to the jump in azimuthal velocity

$$\left(\frac{\partial B_\phi^f}{\partial z} - \frac{\partial B_\phi^i}{\partial z}\right)_{z=z_i} = -\frac{B_z r_i}{\eta}\frac{J_1(\lambda s)}{J_1(c)}\left(\Omega_f - \Omega_i\right), \tag{A8}$$

and where we have used

$$s\Omega_i \approx \frac{J_1(\lambda s)}{J_1(c)} r_i \Omega_i. \tag{A9}$$

Though this last approximation is not very good near $s = r_i$, it allows an exact analytical solution to the problem,

$$B_\phi^f = \frac{B_z r_i^2}{c\eta}\frac{J_1(\lambda s)}{J_1(c)}\mathcal{Z}(z), \tag{A10}$$

$$B_\phi^i = \frac{B_z r_i^2}{c\eta}\frac{J_1(\lambda s)}{J_1(c)}\frac{\sinh(\lambda z)}{\sinh(\lambda z_i)}\mathcal{Z}(z_i), \tag{A11}$$

where

$$\mathcal{Z}(z) = \beta(z)(\Omega_f - \Omega_i) + \frac{2\gamma(z)}{\lambda(z_f - z_i)}\Omega_f, \tag{A12}$$

and

$$\beta(z) = \left[1 - \frac{\tanh(\lambda z)}{\tanh(\lambda z_f)}\right]\cosh(\lambda z)\,\sinh(\lambda z_i), \tag{A13}$$

$$\gamma(z) = -1 + \frac{\cosh(\lambda z)}{\cosh(\lambda z_f)} + \left[\frac{\cosh(\lambda z)}{\cosh(\lambda z_f)} - \frac{\sinh(\lambda z)}{\sinh(\lambda z_f)}\right](\cosh(\lambda z_f)\,\cosh(\lambda z_i) - 1). \tag{A14}$$

Fig. A2 shows the solution obtained when $B_z = 1$ mT, $\eta = 2\ \mathrm{m^2\,s^{-1}}$, $\Omega_f = 0.2^\circ\ \mathrm{yr}^{-1}$ and $\Omega_i = 0^\circ\ \mathrm{yr}^{-1}$. We show the two parts of the solution, corresponding to the β-term and γ-term of (A12). The β-part is the part of B_ϕ produced by the velocity discontinuity at the ICB (from the homogeneous solution), whereas the γ-part is produced by the thermal wind in the fluid (particular solution). Note that we have plotted $-B_\phi$ in Fig. A2(b): the β and γ parts produce opposite contribution to B_ϕ, and hence to the electromagnetic torque.

In order to compute the torque in (A1), we must project the solution at $z = z_i$ to the spherical boundary of the ICB. To do this, we use $s = r_i \sin\theta$, $z_i = r_i \cos\theta$ and also $B_z = B_r \cos\theta$. We also replace B_r in (A1) by $B_r \cos\theta$. With this projection, the torque on the inner core can be written as

$$\Gamma^B_{\mathrm{icb}} = r_i^5 \sigma B_r^2[(\chi_\beta - \chi_\gamma)\Omega_f - \chi_\beta \Omega_i], \tag{A15}$$

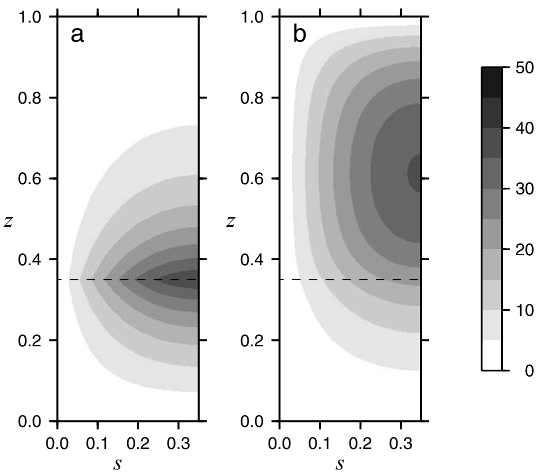

Figure A2. Azimuthal magnetic field inside the tangent cylinder induced by a thermal wind flow profile and computed from (A10) to (A11). (a) B_ϕ due to the jump in velocity at the ICB (β-term in eq. A12); (b) $-B_\phi$ due to the ω-effect of the thermal wind profile (γ-term in eq. A12). Colour scale is in units of mT and distances are dimensionless with $r_f = 1$.

with

$$\chi_\beta = \frac{4\pi}{c}\int_0^{\pi/2} \frac{J_1(c\sin\theta)}{J_1(c)}\beta(\theta)\mathcal{F}(\theta)\sin\theta\, d\theta, \tag{A16}$$

$$\chi_\gamma = -\frac{8\pi}{c^2}\int_0^{\pi/2} \frac{J_1(c\sin\theta)}{J_1(c)(b - \cos\theta)}\gamma(\theta)\mathcal{F}(\theta)\sin\theta\, d\theta, \tag{A17}$$

where $b = r_f/r_i$, $\mathcal{F}(\theta) = \cos^2\theta$ represents the θ-dependence of the square of the radial magnetic field, and $\beta(\theta)$ and $\gamma(\theta)$ are the expressions given by (A13)–(A14) but replacing z with $r_i \cos\theta$. In the absence of gravitational coupling, the largest achievable inner core rotation is obtained by setting (A15) equal to zero, and is determined by

$$\frac{\Omega_i}{\Omega_f} = \frac{\chi_\beta - \chi_\gamma}{\chi_\beta}. \tag{A18}$$

If instead the fluid core were assumed to rotate as a rigid body, then $\chi_\gamma = 0$, and the rotation of the inner core can be entrained at the same rate as Ω_f (Gubbins 1981).

The values of χ_β and χ_γ can be calculated by a numerical integration, and we obtain

$$\chi_\beta = 0.77, \qquad \chi_\gamma = 0.34.$$

With these values, the ratio Ω_i/Ω_f given by (A18) is equal to 0.56. These numerical values should only been considered as plausible estimates. The precise values are highly dependent on the details of the flow and field geometry (e.g. Aurnou *et al.* 1998) and also on the back reaction of the magnetic field on the flow (Hollerbach 1998), which we have neglected here.